(During *et al.*, 2001). However, the mechanism of action of subthalamic stimulation remains to be defined, and the involvement of nonmotor territories may be deleterious. The optimal target site in the STN, where GABA synthesis is enhanced, needs to be identified to ameliorate parkinsonian symptoms while avoiding dyskinesia and cognitive side effects.

Gene therapy using rAAV vectors is now not merely an experimental strategy, but offers a novel and apparently feasible protocol for the treatment of PD.

Acknowledgments

We would like to thank Avigen, Inc., for providing the rAAV vector production system. This study was supported by grants from the Ministry of Health, Labor, and Welfare of Japan; by Strategic Promotion System of Brain Science, in addition to Special Coordination Funds from the Japanese Ministry of Education, Culture, Sports, Science, and Technology; and by The Cell Science Research Foundation.

References

Bankiewicz, K. S., Eberling, J. L., Kohutnicka, M., Jagust, W., Pivirotto, P., Bringas, J., Cunningham, J., Budinger, T. F., and Harvey-White, J. (2000). Convection-enhanced delivery of AAV vector in parkinsonian monkeys; in vivo detection of gene expression and restoration of dopaminergic function using pro-drug approach. *Exp. Neurol.* **164,** 2–14.

Bantel-Schaal, U., Delius, H., Schmidt, R., and zur Hausen, H. (1999). Human adeno-associated virus type 5 is only distantly related to other known primate helper-dependent parvoviruses. *J. Virol.* **73,** 939–947.

Berns, K. I., Bergoin, M., Bloom, M., Lederman, M., Muzyczka, N., Siegl, G., Tal, J., and Tattersall, P. (1995). Family Parvoviridae. *In* "Virus Taxonomy. Classification and Nomenclature of Viruses" (F. A. Murphy *et al.*, Ed.), pp. 169–178. Springer-Verlag, New York.

Bilang-Bleuel, A., Revah, F., Colin, P., Locquet, I., Robert, J. J., Mallet, J., and Horellou, P. (1997). Intrastriatal injection of an adenoviral vector expressing glial-cell-line-derived neurotrophic factor prevents dopaminergic neuron degeneration and behavioral impairment in a rat model of Parkinson disease. *Proc. Natl. Acad. Sci. USA* **94,** 8818–8823.

Bjorklund, A., and Lindvall, O. (2000). Cell replacement therapies for central nervous system disorders. *Nat. Neurosci.* **3,** 537–544.

Bjorklund, A., Kirik, D., Rosenblad, C., Georgievska, B., Lundberg, C., and Mandel, R. J. (2000). Towards a neuroprotective gene therapy for Parkinson's disease: Use of adenovirus, AAV and lentivirus vectors for gene transfer of GDNF to the nigrostriatal system in the rat Parkinson model. *Brain Res.* **886,** 82–98.

Bohn, M. C. (2000). Parkinson's disease: A neurodegenerative disease particularly amenable to gene therapy. *Mol. Ther.* **1,** 494–496.

Brooks, D. J. (2000). Morphological and functional imaging studies on the diagnosis and progression of Parkinson's disease. *J. Neurol.* **247**(Suppl. 2), II 11–18.

Carey, R. J., Pinheiro-Carrera, M., Dai, H., Tomaz, C., and Huston, J. P. (1995). L-DOPA and psychosis: Evidence for L-DOPA-induced increases in prefrontal cortex dopamine and in serum corticosterone. *Biol. Psychiatry* **38,** 669–676.

Chiorini, J. A., Yang, L., Liu, Y., Safer, B., and Kotin, R. M. (1997). Cloning of adeno-associated virus type 4 (AAV4) and generation of recombinant AAV4 particles. *J. Virol.* **71,** 6823–6833.

Chiorini, J. A., Kim, F., Yang, L., and Kotin, R. M. (1999). Cloning and characterization of adeno-associated virus type 5. *J. Virol.* **73,** 1309–1319.

Choi-Lundberg, D. L., Lin, Q., Chang, Y. N., Chiang, Y. L., Hay, C. M., Mohajeri, H., Davidson, B. L., and Bohn, M. C. (1997). Dopaminergic neurons protected from degeneration by GDNF gene therapy. *Science* **275,** 838–841.

Choi-Lundberg, D. L., Lin, Q., Schallert, T., Crippens, D., Davidson, B. L., Chang, Y. N., Chiang, Y. L., Qian, J., Bardwaj, L., and Bohn, M. C. (1998). Behavioral and cellular protection of rat dopaminergic neurons by an adenoviral vector encoding glial cell line-derived neurotrophic factor. *Exp. Neurol.* **154,** 261–275.

Connor, B., Kozlowski, D. A., Schallert, T., Tillerson, J. L., Davidson, B. L., and Bohn, M. C. (1999). Differential effects of glial cell line-derived neurotrophic factor (GDNF) in the striatum and substantia nigra of the aged Parkinsonian rat. *Gene Ther.* **6,** 1936–1951.

Connor, B., Kozlowski, D. A., Unnerstall, J. R., Elsworth, J. D., Tillerson, J. L., Schallert, T., and Bohn, M. C. (2001). Glial cell line-derived neurotrophic factor (GDNF) gene delivery protects dopaminergic terminals from degeneration. *Exp. Neurol.* **169,** 83–95.

Du, B., Wu, P., Boldt-Houle, D. M., and Terwilliger, E. F. (1996). Efficient transduction of human neurons with an adeno-associated virus vector. *Gene Ther.* **3,** 254–261.

Dunnett, S. B., and Bjorklund, A. (1999). Prospects for new restorative and neuroprotective treatments in Parkinson's disease. *Nature* **399,** A32–39.

During, M. J., Samulski, R. J., Elsworth, J. D., Kaplitt, M. G., Leone, P., Xiao, X., Li, J., Freese, A., Taylor, J. R., Roth, R. H., Sladek, J. R., Jr., O'Malley, K. L., and Redmond, D. E., Jr. (1998). In vivo expression of therapeutic human genes for dopamine production in the caudates of MPTP-treated monkeys using an AAV vector. *Gene Ther.* **5,** 820–827.

During, M. J., Kaplitt, M. G., Stern, M. B., and Eidelberg, D. (2001). Subthalamic GAD gene transfer in Parkinson disease patients who are candidates for deep brain stimulation. *Hum. Gene Ther.* **12,** 1589–1591.

Fan, D. S., Ogawa, M., Fujimoto, K. I., Ikeguchi, K., Ogasawara, Y., Urabe, M., Nishizawa, M., Nakano, I., Yoshida, M., Nagatsu, I., Ichinose, H., Nagatsu, T., Kurtzman, G. J., and Ozawa, K. (1998). Behavioral recovery in 6-hydroxydopamine-lesioned rats by cotransduction of striatum with tyrosine hydroxylase and aromatic L-amino acid decarboxylase genes using two separate adeno-associated virus vectors. *Hum. Gene Ther.* **9,** 2527–2535.

Gao, G. P., Alvira, M. R., Wang, L., Calcedo, R., Johnson, J., and Wilson, J. M. (2002). Novel adeno-associated viruses from rhesus monkeys as vectors for human gene therapy. *Proc. Nati. Acad. Sci. USA* **99,** 11854–11859.

Grondin, R., and Gash, D. M. (1998). Glial cell line-derived neurotrophic factor (GDNF): A drug candidate for the treatment of Parkinson's disease. *J. Neurol.* **245,** P35–42.

Hardy, J., Cookson, M. R., and Singleton, A. (2003). Genes and parkinsonism. *Lancet Neurol.* **2,** 221–228.

High, K. A. (2001). AAV-mediated gene transfer for hemophilia. *Ann. N.Y. Acad. Sci.* **953,** 64–74.

Hoshiga, M., Hatakeyama, K., Watanabe, M., Shimada, M., and Kagamiyama, H. (1993). Autoradiographic distribution of [14C]tetrahydrobiopterin and its developmental change in mice. *J. Pharmacol. Exp. Ther.* **267,** 971–978.

Jenner, P. (2000). Factors influencing the onset and persistence of dyskinesia in MPTP-treated primates. *Ann. Neurol.* **47,** S90–99.

Kaddis, F. G., Clarkson, E. D., Weber, M. J., Vandenbergh, D. J., Donovan, D. M., Mallet, J., Horellou, P., Uhl, G. R., and Freed, C. R. (1997). Intrastriatal grafting of Cos cells stably expressing human aromatic L-amino acid decarboxylase: Neurochemical effects. *J. Neurochem.* **68,** 1520–1526.

Kang, U. J., Lee, W. Y., and Chang, J. W. (2001). Gene therapy for Parkinson's disease: Determining the genes necessary for optimal dopamine replacement in rat models. *Hum. Cell* **14,** 39–48.

Kaplitt, M. G., Leone, P., Samulski, R. J., Xiao, X., Pfaff, D. W., O'Malley, K. L., and During, M. J. (1994). Long-term gene expression and phenotypic correction using adeno-associated virus vectors in the mammalian brain. *Nat. Genet.* **8,** 148–154.

Kaspar, B. K., Erickson, D., Schaffer, D., Hinh, L., Gage, F. H., and Peterson, D. A. (2002). Targeted retrograde gene delivery for neuronal protection. *Mol. Ther.* **5,** 50–56.

Kirik, D., Rosenblad, C., Bjorklund, A., and Mandel, R. J. (2000). Long-term rAAV-mediated gene transfer of GDNF in the rat Parkinson's model: Intrastriatal but not intranigral transduction promotes functional regeneration in the lesioned nigrostriatal system. *J. Neurosci.* **20,** 4686–4700.

Kirik, D., Georgievska, B., Burger, C., Winkler, C., Muzyczka, N., Mandel, R. J., and Bjorklund, A. (2002). Reversal of motor impairments in parkinsonian rats by continuous intrastriatal delivery of L-dopa using rAAV-mediated gene transfer. *Proc. Natl. Acad. Sci. USA* **99,** 4708–4713.

Klein, R. L., Lewis, M. H., Muzyczka, N., and Meyer, E. M. (1999). Prevention of 6-hydroxydopamine-induced rotational behavior by BDNF somatic gene transfer. *Brain Res.* **847,** 314–320.

Kordower, J. H., Palfi, S., Chen, E. Y., Ma, S. Y., Sendera, T., Cochran, E. J., Mufson, E. J., Penn, R., Goetz, C. G., and Comella, C. D. (1999). Clinicopathological findings following intraventricular glial-derived neurotrophic factor treatment in a patient with Parkinson's disease. *Ann. Neurol.* **46,** 419–424.

Kordower, J. H., Emborg, M. E., Bloch, J., Ma, S. Y., Chu, Y., Leventhal, L., McBride, J., Chen, E. Y., Palfi, S., Roitberg, B. Z., Brown, W. D., Holden, J. E., Pyzalski, R., Taylor, M. D., Carvey, P., Ling, Z., Trono, D., Hantraye, P., Deglon, N., and Aebischer, P. (2000). Neurodegeneration prevented by lentiviral vector delivery of GDNF in primate models of Parkinson's disease. *Science* **290,** 767–773.

Kozlowski, D. A., Connor, B., Tillerson, J. L., Schallert, T., and Bohn, M. C. (2000). Delivery of a GDNF gene into the substantia nigra after a progressive 6-OHDA lesion maintains functional nigrostriatal connections. *Exp. Neurol.* **166,** 1–15.

Lange, H., Thorner, G., Hopf, A., and Schroder, K. F. (1976). Morphometric studies of the neuropathological changes in choreatic diseases. *J. Neurol. Sci.* **8,** 401–425.

Langston, J. W., Quik, M., Petzinger, G., Jakowec, M., and Di Monte, D. A. (2000). Investigating levodopa-induced dyskinesias in the parkinsonian primate. *Ann. Neurol.* **47,** S79–89.

Leff, S. E., Spratt, S. K., Snyder, R. O., and Mandel, R. J. (1999). Long-term restoration of striatal L-aromatic amino acid decarboxylase activity using recombinant adeno-associated viral vector gene transfer in a rodent model of Parkinson's disease. *Neuroscience* **92,** 185–196.

Levine, R. A., Miller, L. P., and Lovenberg, W. (1981). Tetrahydrobiopetrin in striatum: localization in dopamine nerve terminals and role in catecholamine synthesis. *Science* **214,** 919–921.

Lieberman, D. M., Laske, D. W., Morrison, P. F., Bankiewicz, K. S., and Oldfield, E. H. (1995). Convection-enhanced distribution of large molecules in gray matter during interstitial drug infusion. *J. Neurosurg.* **82,** 1021–1029.

Mandel, R. J., Spratt, S. K., Snyder, R. O., and Leff, S. E. (1997). Midbrain injection of recombinant adeno-associated virus encoding rat glial cell line-derived neurotrophic factor protects nigral neurons in a progressive 6-hydroxydopamine-induced degeneration model of Parkinson's disease in rats. *Proc. Natl. Acad. Sci. USA* **94,** 14083–14088.

Mandel, R. J., Rendahl, K. G., Spratt, S. K., Snyder, R. O., Cohen, L. K., and Leff, S. E. (1998). Characterization of intrastriatal recombinant adeno-associated virus-mediated gene transfer of

human tyrosine hydroxylase and human GTP-cyclohydrolase I in a rat model of Parkinson's disease. *J. Neurosci.* **18,** 4271–4284.

Mandel, R. J., Snyder, R. O., and Leff, S. E. (1999). Recombinant adeno-associated viral vector-mediated glial cell line-derived neurotrophic factor gene transfer protects nigral dopamine neurons after onset of progressive degeneration in a rat model of Parkinson's disease. *Exp. Neurol.* **160,** 205–214.

Matsushita, T., Elliger, S., Elliger, C., Podsakoff, G., Villarreal, L., Kurtzman, G. J., Iwaki, Y., and Colosi, P. (1998). Adeno-associated virus vectors can be efficiently produced without helper virus. *Gene Ther.* **5,** 938–945.

Miller, D. G., Rutledge, E. A., and Russell, D. W. (2002). Chromosomal effects of adeno-associated virus vector integration. *Nat. Genet.* **30,** 147–148.

Mochizuki, H., Hayakawa, H., Migita, M., Shibata, M., Tanaka, R., Suzuki, A., Shimo-Nakanishi, Y., Urabe, T., Yamada, M., Tamayose, K., Shimada, T., Miura, M., and Mizuno, Y. (2001). An AAV-derived Apaf-1 dominant negative inhibitor prevents MPTP toxicity as antiapoptotic gene therapy for Parkinson's disease. *Proc. Natl. Acad. Sci. USA* **98,** 10918–10923.

Muramatsu, S., Mizukami, H., Young, N. S., and Brown, K. E. (1996). Nucleotide sequencing and generation of an infectious clone of adeno-associated virus 3. *Virology* **221,** 208–217.

Muramatsu, S., Fujimoto, K., Ikeguchi, K., Shizuma, N., Kawasaki, K., Ono, F., Shen, Y., Wang, L., Mizukami, H., Kume, A., Matsumura, M., Nagatsu, I., Urano, F., Ichinose, H., Nagatsu, T., Terao, K., Nakano, I., and Ozawa, K. (2002). Behavioral recovery in a primate model of Parkinson's disease by triple transduction of striatal cells with adeno-associated viral vectors expressing dopamine-synthesizing enzymes. *Hum. Gene Ther.* **13,** 345–354.

Nagatsu, I., Arai, R., Sakai, M., Yamawaki, Y., Takeuchi, T., Karasawa, N., and Nagatsu, T. (1997). Immunohistochemical colocalization of GTP cyclohydrolase I in the nigrostriatal system with tyrosine hydroxylase. *Neurosci. Lett.* **224,** 185–188.

Nagatsu, T., and Ichinose, H. (1999). Molecular biology of catecholamine-related enzymes in relation to Parkinson's disease. *Cell. Mol. Neurobiol.* **19,** 57–66.

Nagatsu, T., Horikoshi, T., Sawada, M., Nagatsu, I., Kondo, T., Iizuka, R., and Narabayashi, H. (1987). Biosynthesis of tetrahydrobiopterin in parkinsonian human brain. *Adv. Neurol.* **45,** 223–226.

Nakamura, K., Ahmed, M., Barr, E., Leiden, J. M., and Kang, U. J. (2000). The localization and functional contribution of striatal aromatic L-amino acid decarboxylase to L-3,4-dihydroxyphenylalanine decarboxylation in rodent parkinsonian models. *Cell Transplant* **9,** 567–576.

Natsume, A., Mata, M., Goss, J., Huang, S., Wolfe, D., Oligino, T., Glorioso, J., and Fink, D. J. (2001). Bcl-2 and GDNF delivered by HSV-mediated gene transfer act additively to protect dopaminergic neurons from 6-OHDA-induced degeneration. *Exp. Neurol.* **169,** 231–238.

Rutledge, E. A., Halbert, C. L., and Russell, D. W. (1998). Infectious clones and vectors derived from adeno-associated virus (AAV) serotypes other than AAV type 2. *J. Virol.* **72,** 309–319.

Sanchez-Pernaute, R., Harvey-White, J., Cunningham, J., and Bankiewicz, K. S. (2001). Functional effect of adeno-associated virus mediated gene transfer of aromatic L-amino acid decarboxylase into the striatum of 6-OHDA-lesioned rats. *Mol. Ther.* **4,** 324–330.

Shen, Y., Muramatsu, S. I., Ikeguchi, K., Fujimoto, K. I., Fan, D. S., Ogawa, M., Mizukami, H., Urabe, M., Kume, A., Nagatsu, I., Urano, F., Suzuki, T., Ichinose, H., Nagatsu, T., Monahan, J., Nakano, I., and Ozawa, K. (2000). Triple transduction with adeno-associated virus vectors expressing tyrosine hydroxylase, aromatic-L-amino-acid decarboxylase, and GTP cyclohydrolase I for gene therapy of Parkinson's disease. *Hum. Gene Ther.* **11,** 1509–1519.

Srivastava, A., Lusby, E. W., and Berns, K. I. (1983). Nucleotide sequence and organization of the adeno-associated virus 2 genome. *J. Virol.* **45,** 555–564.

Wachtel, S. R., Bencsics, C., and Kang, U. J. (1997). Role of aromatic L-amino acid decarboxylase for dopamine replacement by genetically modified fibroblasts in a rat model of Parkinson's disease. *J. Neurochem.* **69,** 2055–2063.

Walton, K. M. (1999). GDNF: A novel factor with therapeutic potential for neurodegenerative disorders. *Mol. Neurobiol.* **19,** 43–59.

Wang, L., Muramatsu, S., Lu, Y., Ikeguchi, K., Fujimoto, K., Okada, T., Mizukami, H., Hanazono, Y., Kume, A., Urano, F., Ichinose, H., Nagatsu, T., Nakano, I., and Ozawa, K. (2002). Delayed delivery of AAV-GDNF prevents nigral neurodegeneration and promotes functional recovery in a rat model of Parkinson's disease. *Gene Ther.* **9,** 381–389.

Xiao, W., Chirmule, N., Berta, S. C., McCullough, B., Gao, G., and Wilson, J. M. (1999). Gene therapy vectors based on adeno-associated virus type 1. *J. Virol.* **73,** 3994–4003.

Zhong, X. H., Haycock, J. W., Shannak, K., Robitaille, Y., Fratkin, J., Koeppen, A. H., Hornykiewicz, O., and Kish, S. J. (1995). Striatal dihydroxyphenylalanine decarboxylase and tyrosine hydroxylase protein in idiopathic Parkinson's disease and dominantly inherited olivopontocerebellar atrophy. *Mov. Disord.* **10,** 10–17.

doi:10.1016/j.ymthe.2003.08.019

ARTICLE

Persistent Phenotypic Correction of Central Diabetes Insipidus Using Adeno-associated Virus Vector Expressing Arginine–Vasopressin in Brattleboro Rats

Junichi Ideno,[1,2] Hiroaki Mizukami,[1] Kazufumi Honda,[2] Takashi Okada,[1] Yutaka Hanazono,[1] Akihiro Kume,[1] Toshikazu Saito,[3] Shun Ishibashi,[2] and Keiya Ozawa[1,†]

[1]*Division of Genetic Therapeutics, Center for Molecular Medicine and* [2]*Division of Endocrinology and Metabolism, Jichi Medical School, Tochigi 329-0498, Japan*
[3]*Social Insurance Chuo General Hospital, Tokyo 169-0073, Japan*

[†]*To whom correspondence and reprint requests should be addressed at the Division of Genetic Therapeutics, Center for Molecular Medicine, Jichi Medical School, 3311-1 Yakushiji, Minamikawachi-machi, Kawachi-gun, Tochigi 329-0498, Japan. Fax: +81-285-44-8675. E-mail: kozawa@ms.jichi.ac.jp.*

Adeno-associated virus (AAV) vector is suitable for gene transfer to the central nervous system. However, the efficacy of gene therapy for neuroendocrine disease is still unknown. In this study, we injected AAV vector encoding arginine–vasopressin (AVP) stereotaxically into the bilateral hypothalamus of Brattleboro rats. Brattleboro rats show a central diabetes insipidus (CDI) phenotype and growth retardation due to a complete deficiency of AVP. Following injection, both urine volume and urine osmolality normalized, and these therapeutic effects persisted for more than 50 weeks. In addition to phenotypic correction, secretion of transgene-derived AVP was enhanced after 24 h water deprivation or hypertonic saline injection, and water diuresis was demonstrated after acute water loading. Also, reduced body weight and low plasma insulin-like growth factor I levels of Brattleboro rats were restored after AVP gene transduction, suggesting the importance of AVP in growth. These findings indicate that hypothalamic neurons of Brattleboro rats can produce and release mature AVP following AAV-mediated gene transduction, resulting in long-term phenotypic correction of CDI. Moreover, the fact that transgene-derived AVP was secreted adequately in response to stimuli, even if it was expressed constitutively, suggests advantages of gene therapy for neuroendocrine diseases and offers a basis to investigate AVP function.

Key Words: adeno-associated virus vector, gene therapy, arginine–vasopressin, central diabetes insipidus, insulin-like growth factor I, central nervous system

INTRODUCTION

The central nervous system (CNS) is one of the major target organs for gene therapy, and successful gene transfer to the CNS has been reported using various vectors including adenovirus vectors [1–4], adeno-associated virus (AAV) vectors [5,6], and lentiviral vectors [7]. Moreover, some studies have demonstrated that CNS gene therapy restored brain function in animal models [5,8–11]. However, it is usually difficult to estimate transgene expression by noninvasive observations because of the complexity of brain functions. The Brattleboro rat is a suitable model for CNS gene therapy with its simple phenotype of central diabetes insipidus (CDI) [12]. It does not synthesize functional arginine–vasopressin (AVP) and shows CDI, which is characterized by polyuria and diluted urine excretion [13]. Therefore the degree of transgene expression can be estimated by urine volume and osmolality.

The antidiuretic hormone AVP acts on the collecting tubule in the kidney for water reabsorption, and plasma AVP levels are strictly regulated by plasma osmolality and blood volume [14–17]. AVP is primarily synthesized in the supraoptic nucleus (SON) and paraventricular nucleus (PVN) of the hypothalamus as a precursor that consists of a signal peptide, AVP, carrier protein neurophysin, and glycopeptide [18]. The AVP precursor is enzymatically processed into mature AVP, which is stored in the neurohypophysis and released into circulation in response to stimuli [19]. The deficiency of functional AVP in Brattleboro rats is due to a single base deletion in the coding region, which leads to the loss of a normal stop codon

1525-0016/03 $30.00

doi:10.1016/j.ymthe.2003.08.019

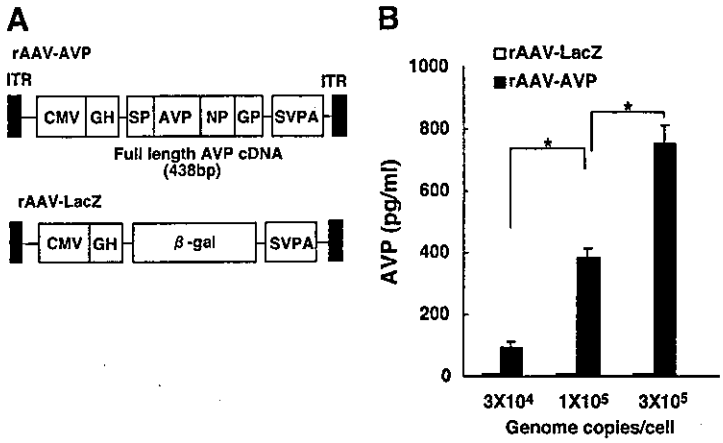

FIG. 1. Structure of rAAV vector and *in vitro* AVP production. (A) Schematic structure of rAAV-AVP and rAAV-LacZ. ITR, inverted terminal repeat; CMV, human cytomegalovirus promoter; GH, human growth hormone first intron enhancer; SP, signal peptide; AVP, arginine-vasopressin; NP, neurophysin; GP, glycoprotein; SVPA, SV40 poly(A); β-gal, β-galactosidase. (B) Forty-eight hours after rAAV vector transduction, AVP concentration of culture supernatant was measured by RIA. Statistical analysis (ANOVA) revealed that transduction of 293 cells with increasing doses of rAAV-AVP resulted in a dose-dependent increase in the AVP concentration of the culture supernatant, while transduction of 293 cells with rAAV-LacZ resulted in small amounts of AVP. $*P < 0.05$. Data represent means ± SD, $n = 6$ at each dose.

[20]. Some studies showed that the injection of AVP mRNA into the hypothalamus transiently corrected CDI in Brattleboro rats [21,22], and Geddes *et al.* reported that production of AVP and partial correction of CDI was achieved by the injection of an AVP gene-encoding adenovirus vector into the hypothalamus of Brattleboro rats [23]. Moreover, long-term CDI correction of Brattleboro rats has recently been demonstrated using a lentiviral vector [24]. However, the function and kinetics of transgene-derived AVP were not investigated in these models.

We used an AAV vector as a vehicle for gene transfer to the CNS. The AAV vector is attractive for use in gene therapy because it has advantages over other viral and nonviral gene delivery systems with regard to safety, efficacy, and duration of action [8,9,11,25]. In the present study, we examined the effect of CNS gene therapy in Brattleboro rats using an AAV vector encoding an AVP gene (rAAV-AVP) and investigated the kinetics and action of transgene-derived AVP.

RESULTS

Confirmation of Vector Integrity

We measured the concentration of AVP in the culture supernatant after transduction of 293 cells with AAV vectors. In the rAAV-AVP group, AVP levels of the culture supernatant were dose-dependent on the rAAV-AVP, while they remained at background values in the rAAV vector encoding a β-galactosidase gene (rAAV-LacZ) group (Fig. 1B).

Phenotypic Changes in Brattleboro Rats

Brattleboro rats show polyuria and diluted urine excretion because of a deficiency of AVP. Therefore, the degree of AVP gene expression can be estimated by examining urine volume and osmolality. After an injection of the rAAV-AVP vector into the bilateral SON of Brattleboro rats, urine volume markedly decreased (Fig. 2A) and urine osmolality elevated to normal levels in the rats that received rAAV-AVP (AVP-treated group), while these parameters remained unchanged in the rats that received rAAV-LacZ (control group) (Fig. 2B). The effect of CDI correction persisted for more than 60 weeks.

Immunohistochemistry

Fig. 3 shows immunohistochemistry of AVP at the SON. Black spots, which were carbon particles included in the vector solution, reflect the penetration following vector injection. While the control group had no staining (Figs. 3A and 3B), the AVP-treated group had numerous AVP-positive neurons that were stained brown, and the distribution of these neurons was localized in the SON (Figs.

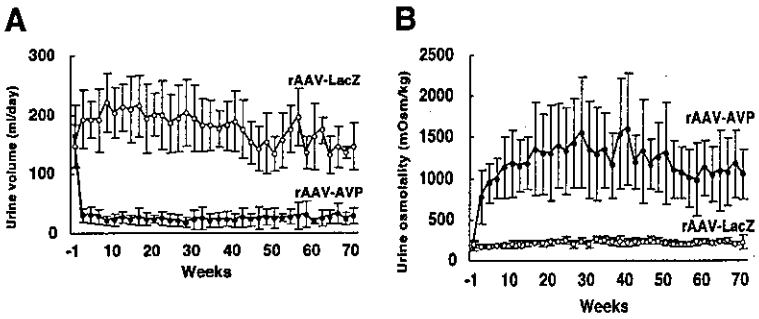

FIG. 2. Time course of (A) urine volume and (B) urine osmolality. Urine was collected every 2 weeks after an injection of rAAV-AVP (filled circles) or rAAV-LacZ (empty circles) into the supraoptic nucleus of Brattleboro rats. Statistical analysis (repeated-measure ANOVA) revealed that an injection of rAAV-AVP corrected central diabetes insipidus for more than 60 weeks. All rats had free access to water and food. Data represent means ± SD, $n = 7$–9 rats in each group, at each time point.

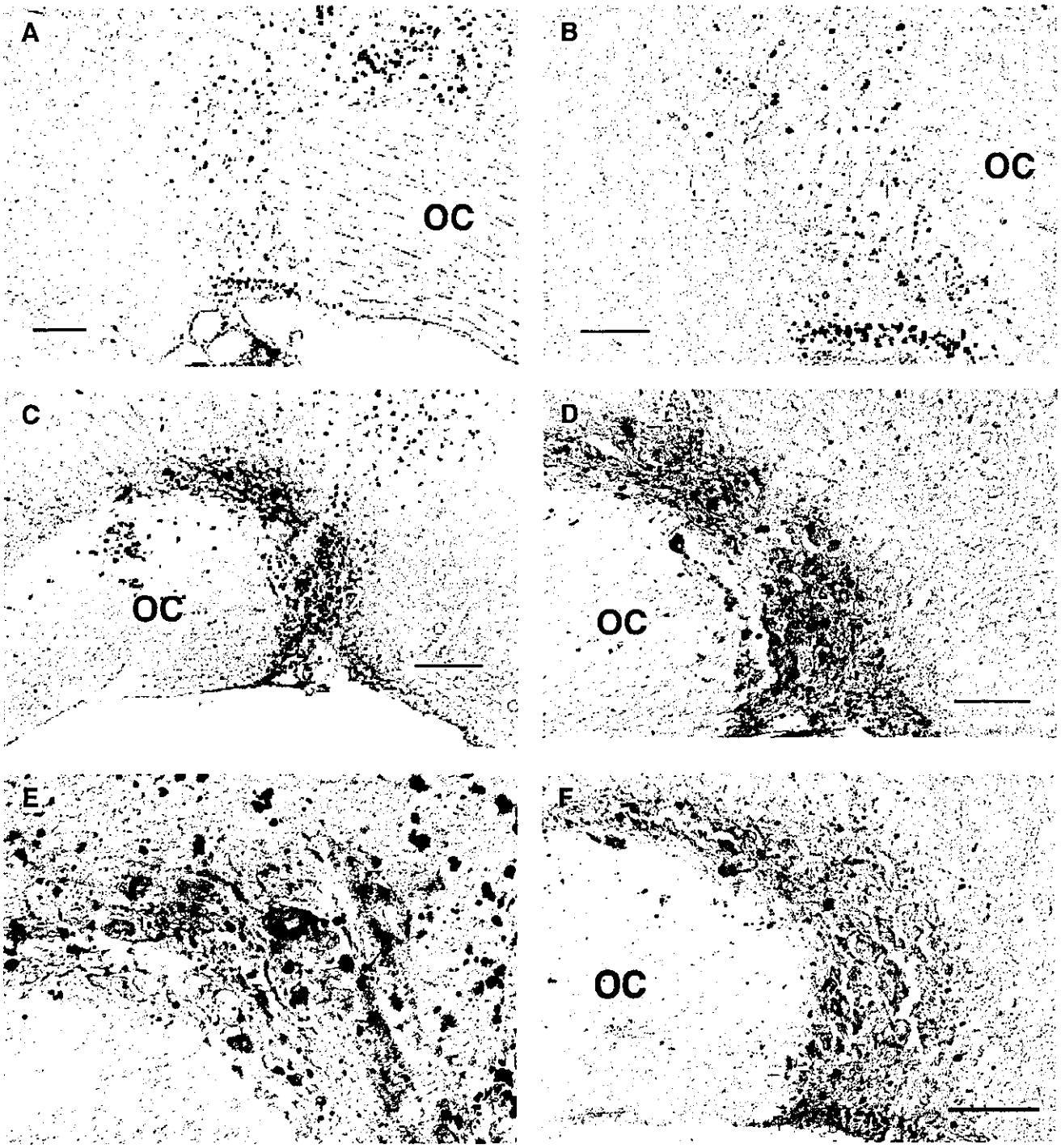

FIG. 3. AVP immunohistochemistry at the supraoptic nucleus (SON) of Brattleboro rats. (A and B) rAAV-LacZ-treated rat and (C, D, E, and F) rAAV-AVP-treated rat. The brain was removed 10 weeks after vector injection (A, B, C, D, and E) or 70 weeks after vector injection (F). AVP-positive magnocellular neurons that stained brown are detected in the SON of the rAAV-AVP-treated Brattleboro rats, while there were no AVP-positive cells in the rAAV-LacZ-treated rats. Black spots are carbon particles included in the vector solution. (A and C) Bar, 100 μm. (B, D, and F) Bar, 40 μm. OC, optic chiasma.

doi:10.1016/j.ymthe.2003.08.019

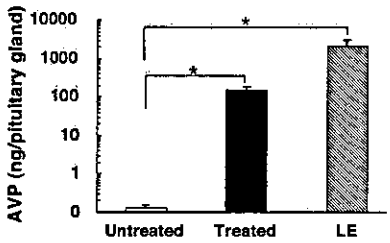

FIG. 4. AVP content of neurohypophysis. AVP was extracted after homogenization of the neurohypophysis and AVP levels were determined by RIA. Neurohypophysis was removed 10 weeks after rAAV-AVP injection into the supraoptic nucleus of Brattleboro rats (treated). The untreated Brattleboro rats were used as a negative control and the Long-Evans rats (LE) were used as a positive control. *$P < 0.05$ compared to the untreated rats. Data represent the means ± SD, $n = 6$ rats in each group.

3C, 3D, and 3E). Fig. 3F shows AVP-positive neurons in the SON 70 weeks after rAAV-AVP administration.

AVP Content of Neurohypophysis

To clarify the storage of the transgene-derived AVP, we measured AVP content of the neurohypophysis by radioimmunoassay (RIA). In the AVP-treated group, neurohypophyseal extracts contained about 10% AVP of the Long-Evans (LE) rats, the maternal strain of Brattleboro rats. The untreated Brattleboro rats (untreated group) were used as a negative control to estimate the kinetics of transgene-derived AVP because the CDI phenotype of the Brattleboro rats did not change after rAAV-LacZ administration. They showed negligible amount of AVP in the neurohypophysis (Fig. 4).

Plasma Osmolality and AVP

Fig. 5A shows basal levels of plasma AVP and osmolality. In the AVP-treated group, plasma osmolality was decreased and plasma levels of AVP were elevated in comparison with the untreated group. After 24-h water deprivation, plasma levels of AVP were elevated in the AVP-treated group while unchanged in the untreated group (3.9 ± 2.5 and 0.23 ± 0.21 pg/ml, respectively, $P < 0.05$; Fig. 5B). Hypertonic saline test was performed to estimate the secretion of transgene-derived AVP for osmotic stimulus. After an injection of hypertonic saline, plasma osmolality was elevated over 330 mosmol/kg H_2O (data not shown). Plasma AVP level was elevated in accordance with the rise in plasma osmolality specifically in the AVP-treated group (Fig. 6).

Acute Water Loading Test

The increase in blood volume inhibits AVP release from neurohypophysis via the negative feedback mechanisms of AVP. To estimate this mechanism in the AVP-treated group, we examined acute water loading. After water loading, urine volume increased (Fig. 7A) and diluted urine was excreted (Fig. 7B) in 4 h in the AVP-treated group. These responses of urine volume and osmolality for water loading were similar to those of the wild-type rats.

Body Weight and Plasma Insulin-like Growth Factor I (IGF-I)

Fig. 8A shows the changes in body weight. Body weight gain in the AVP-treated group was significantly greater than that of the control group, which remained lean throughout the observation period. However, food intake was not significantly different between these two groups (Fig. 8B). Plasma IGF-I levels of the AVP-treated group were significantly higher than those of the untreated group (Fig. 8D). On the other hand, plasma IGF-I levels in Brattleboro rats that received DDAVP, an AVP V2 receptor agonist, were not different from those in the untreated rats.

DISCUSSION

In this study, we demonstrated that the rAAV-AVP vector injected into the SON ameliorated the CDI of Brattleboro rats, and the secretion of transgene-derived AVP was regulated by physiological stimuli. The AVP gene expression was sufficient to normalize water metabolism and lasted for more than 60 weeks. Other studies also demonstrated that long-term transgene expression was achieved by rAAV vector-mediated gene transduction into the CNS

FIG. 5. Plasma osmolality and plasma AVP concentration. (A) Freely water drinking rats and (B) rats deprived water for 24 h were studied. Rats were decapitated rAAV-AVP 10 weeks after injection into the supraoptic nucleus of Brattleboro rats (filled circles). Age-matched untreated Brattleboro rats (empty circles) were used as a negative control and age-matched Long-Evans rats (empty triangles) were used as a positive control.

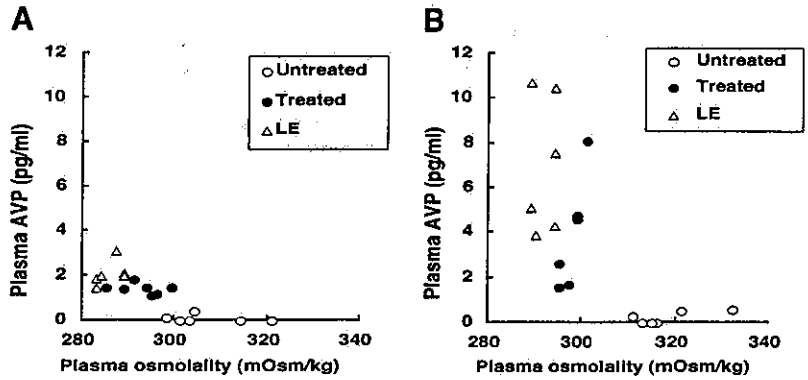

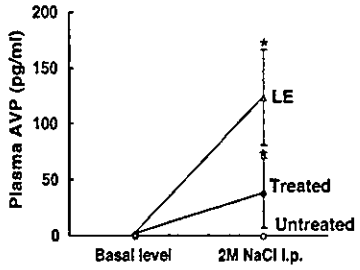

FIG. 6. Hyperosmotic saline test. Hyperosmotic saline (2 M NaCl, 1 ml/100 g body weight) was injected intraperitoneally to elevate plasma AVP concentration. Thirty minutes after injection, rats were decapitated, and plasma AVP levels were measured by RIA (2 M NaCl ip). Plasma AVP levels were compared with those of freely water drinking rats (basal level). This experiment was performed 10 weeks after rAAV-AVP injection into the supraoptic nucleus of Brattleboro rats (filled circles). Untreated Brattleboro rats (empty circles) were used as a negative control and Long-Evans rats (empty triangles) were used as a positive control. *$P < 0.05$ compared to the basal level. Data represent means ± SD, $n = 6$ rats in all groups, at each time point.

[9,11]. The rAAV vector is derived from a nonpathogenic virus [25], and no cytotoxicity was reported at the injection site [11]. Therefore, the rAAV vector is a suitable vehicle for gene therapy of the CNS.

In addition to the CDI phenotype, the Brattleboro rats show growth retardation and are smaller than age-matched LE rats. Our results demonstrated that the AVP-treated group gained more body weight than the control group despite no difference in food intake. Plasma IGF-I level of untreated rats was significantly lower than that of the LE rats, while plasma IGF-I level of the AVP-treated group was normalized. These results are consistent with an observation that exogenous AVP supplement resulted in body weight increase in Brattleboro rats [26]. A previous study demonstrated that the growth retardation in Brattleboro rats was attributed to a decrease in hepatic growth hormone (GH) receptors and low plasma somatomedin activity without the reduction in GH secretion [27]. Administration of DDAVP, an AVP V2 receptor agonist, could not increase plasma IGF-I levels of Brattleboro rats in this study. These findings suggested that circulating AVP is related to body weight increase via the AVP V1a receptor.

AVP-positive cells were detected in the SON of only the AVP-treated rats, while there were no AVP-positive cells in control rats detected using antiserum recognizing AVP in its processed form [28]. These results showed that transgene-derived AVP was specifically produced in the SON of AVP-treated rats, but the surrounding tissue of the SON could not produce mature AVP despite a leakage of the vector solution. A processing enzyme is essential to produce mature AVP [29], and we suppose that this is the major reason for SON-specific AVP production. We could not exclude the possibility that glial cells produced transgene-derived AVP in this study. However, we suppose that the majority of the transgene-derived AVP was produced by magnocellular neurons in the SON because previous studies have characterized the cell types transduced after parenchymal injection of rAAV as predominantly neurons [9,30], and glial cells could not release AVP into the circulation even if they could produce mature AVP. Magnocellular neurons of the SON are divided into two groups, AVP-producing neurons and oxytocin-producing neurons. Oxytocin-producing neurons have processing enzyme to produce mature AVP and could release secretory granule in response to osmotic stimulation [31]. Therefore, we could not estimate which neurons produced transgene-derived AVP in this study. AVP is primarily produced at two nuclei, the SON and the PVN, but AVP function in these nuclei may be different [32–36]. Further analysis of our model may reveal the AVP function in the SON.

In the analysis of AVP content in various tissues, significant amounts of AVP were detected in the SON, neurohypophysis, and circulating blood in the AVP-treated group. Moreover, plasma AVP levels were sufficient to normalize CDI, and urinary AVP excretion was the same level as that of the wild-type rats (urinary AVP excretion; 872 ± 249 pg/day in the AVP-treated group and 924 ± 258 pg/day in the wild-type rats, $P = 0.39$). However,

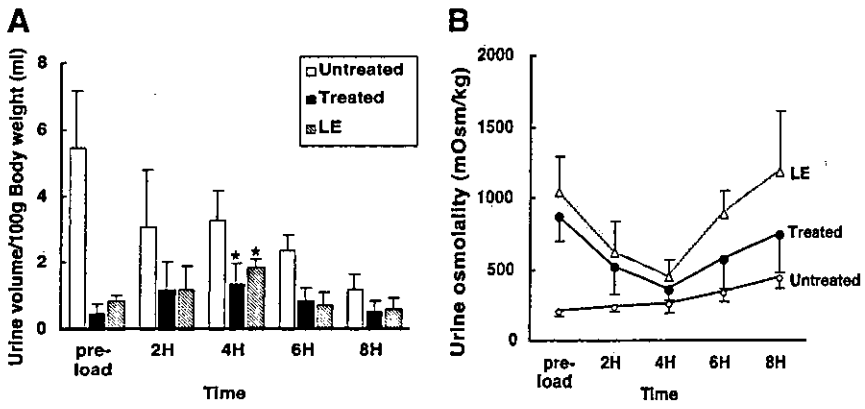

FIG. 7. Acute water loading test. Distilled water (4 ml/100 g body weight) was injected intraperitoneally to inhibit AVP release from the neurohypophysis. (A) Urine volume and (B) urine osmolality were measured every 2 h in untreated Brattleboro rats, rAAV-AVP-treated Brattleboro rats, and Long-Evans (LE) rats. After water loading, urine volume increased and urine osmolality was decreased in the rAAV-AVP-treated Brattleboro rats and the LE rats. *$P < 0.05$ compared to pre-water loading. Data represent means ± SD, $n = 6$ in all groups, at each time point.

doi:10.1016/j.ymthe.2003.08.019

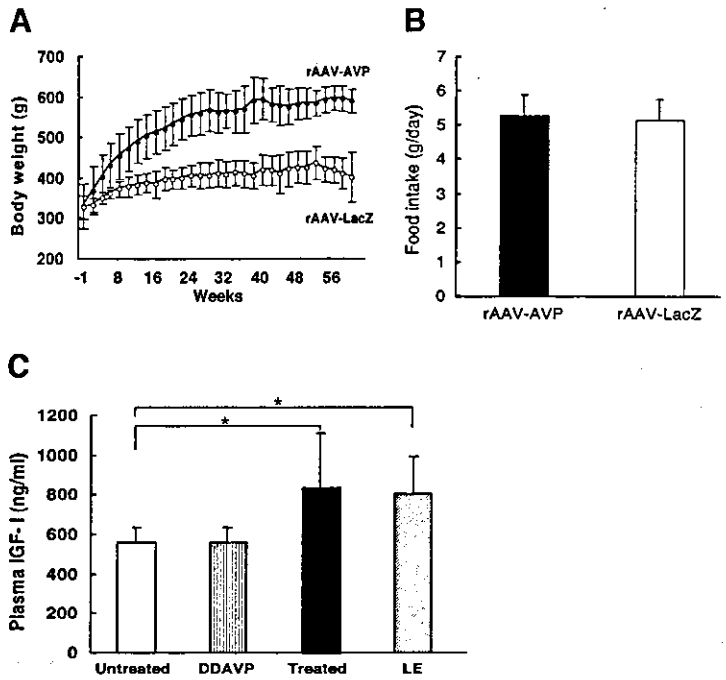

FIG. 8. AVP increases body weight and plasma IGF-I. (A) Time course of body weight change in rAAV-AVP-treated Brattleboro rats (filled circles) or rAAV-LacZ-treated Brattleboro rats (empty circles). Statistical analysis (repeated-measure ANOVA) revealed that the body weight of AVP-treated rats increased more than that of control rats. Data represent means ± SD, n = 7–9 rats in each group, at each time point. (B) Food intake for 24 h was measured in both AVP-treated rats and control rats. Food intake was expressed as g/100 g body weight 8 weeks after vector injection. There was no significant difference between two groups. Data represent means ± SD, n = 7–9 rats in each group. (C) Plasma IGF-I levels were measured by RIA. The AVP-treated rats were decapitated 10 weeks after rAAV-AVP administration (treated). The untreated Brattleboro rats were used as a negative control and the Long-Evans rats (LE) were used as a positive control. The DDAVP rats received DDAVP at the rate of 4 ng/h to normalize polydipsia in Brattleboro rats. Statistical analysis (ANOVA) revealed that plasma IGF-I levels of AVP-treated rats were higher than those of DDAVP rats. *P < 0.05 compared to the untreated rats. Data represent the means ± SD, n = 6–9 rats.

plasma AVP levels of AVP-treated group after 24-h water deprivation or hyperosmotic saline injection were slightly lower than those of the wild-type rats. AVP content of the neurohypophysis in the AVP-treated group was approximately 1/10 of that in the wild-type rats, and we supposed this was a major reason for decreasing response of transgene-derived AVP. These observations suggest that only a part of the AVP stored in the neurohypophysis contributes to water metabolism under physiological conditions. The total amount of neurohypophyseal AVP is enormous in wild-type rats [37], and that is divided into two types, the release pool and storage pool [38]. Our findings may contribute to further study that estimates the function of AVP stored in the neurohypophysis.

In the AVP-treated group, the release of transgene-derived AVP was enhanced in response to water deprivation and hypertonic saline injection. Moreover, it is suggested that water administration inhibits transgene-derived AVP secretion because water diuresis was demonstrated after water loading. These results suggest that the secretion of transgene-derived AVP is regulated by the stimuli and similar to that of the wild-type rats. In the wild-type rats, AVP production is regulated via the stimulus–transcription coupling [39] and there is coordination between AVP secretion and AVP transcription [40,41]. The 5′ regulatory region of the AVP gene is essential to regulate AVP production. However, the production of transgene-derived AVP was not regulated in this study because AVP cDNA lacked the 5′ regulatory region and was driven by a constitutive cytomegalovirus (CMV) promoter. We suppose that the plasma level of transgene-derived AVP is regulated at AVP release in the neurohypophysis. Previous studies demonstrated that there was a stimulus–secretion coupling in AVP release [42], and the electrical properties of secretory cells in the Brattleboro rat were similar to those of normal rats [43]. These findings imply that the secretion of transgene-derived AVP is also coupled with the stimulus and regulated in response to stimuli despite the lack of 5′ regulatory region. This model suggests that the strict regulation of transgene expression is not a prerequisite and gene therapy for neuroendocrine disease is feasible if neuroendocrine cells are remaining.

In conclusion, rAAV-mediated CNS gene transfer resulted in phenotypic correction of CDI in Brattleboro rats for more than 60 weeks. The secretion of transgene-derived AVP was regulated by feedback mechanisms although the AVP transgene was driven by the constitutive promoter. These findings provide a new approach to gene therapy for neuroendocrine disease and offer a basis to investigate physiological function of AVP.

Materials and Methods

AAV vector production. The rAAV (type 2) vector structure is depicted diagrammatically in Fig. 1A. The rAAV-AVP contains the wild-type AVP cDNA (provided by Dr. Hartwig Schmale and Dr. Dietmar Richter, University of Hamburg, Hamburg, Germany) with the human CMV immediate-early promoter, human GH first intron enhancer, and simian virus 40 polyadenylation signal sequence between the inverted terminal repeats of the AAV genome. The rAAV was produced according to the helper-free system [44]. The vector was purified twice by cesium chloride gradient ultracentrifugation, and the titer was determined by quantitative DNA

dot-blot hybridization of DNase 1-treated vector stocks. A rAAV-LacZ was also prepared and used as a control. The vector integrity was confirmed by measuring AVP levels of the culture supernatant 48 h after transduction of 293 cells.

Animals. Male homozygous Brattleboro rats and LE rats (300–400 g body weight) were used in this study. Both strains of rats were bred in the Jichi Medical School vivarium. They were housed in an air-conditioned room with a controlled light cycle (lights on between 0730 and 1930 h). Access to food and water was not restricted. All experiments were performed in accordance with the guidelines for animal care at the Jichi Medical School.

rAAV vector administration to Brattleboro rats. Each Brattleboro rat received 3 μl (1×10^{10} genome copies/μl) of either rAAV-AVP vector or rAAV-LacZ vector into the bilateral SON via a rat stereotaxic apparatus (coordinates: *x*, 1.6 mm; *y*, 1.4 mm; *z*, 9.2 mm from Bregma, according to Paxinos and Watson [45]) under pentobarbital anesthesia. The vector solution was injected over 10 min using a microinjection apparatus (IC3210; Kd Scientific, Boston, MA). To certify the injection of vector into the SON, carbon particles were added to the vector solution. Rats were raised in individual cages, and body weight and urine volume were measured every 2 weeks using a rat metabolic cage (KN-649; Natume Seisakusho Co., Tokyo, Japan).

Basal characteristics and water deprivation test. Ten weeks after vector injection, the AVP-treated rats were divided randomly into two groups, a freely water drinking group and a 24-h water deprivation group. Rats were decapitated, and blood was collected from the trunk into a tube containing EDTA–Na. The brain and neurohypophysis were separated immediately. The brain was stored after fixation in paraformaldehyde. The neurohypophysis was boiled for 10 min in 1 ml of a 1 M acetic acid–20 mM sodium chloride solution to deactivate endogenous protease and then homogenized. The supernatant was stored at −80°C until assay. The untreated group was used as a negative control.

Hypertonic saline test. The AVP-treated group, the untreated group, and the LE rats received a hypertonic saline solution (2 M, 1 ml/100 g body weight) intraperitoneally. Following an injection, access to food and water was restricted. Thirty minutes later, rats were decapitated and blood was collected from the trunk and analyzed for plasma osmolality and AVP.

Acute water loading test. The AVP-treated group, the untreated group, and the LE rats received 4 ml/100 g body weight of distilled water intraperitoneally. Access to food and water was restricted after an injection. Urine was collected every 2 h for 8 h to determine urine volume and osmolality.

Animal treatment for IGF-I measurement. Brattleboro rats received DDAVP, an AVP V2 receptor agonist, at the rate of 4 ng/h subcutaneously, using a mini osmotic pump (Model 2004, Alzet, Cupertino, CA), to correct polydipsia. The rats were provided with free access to food and water for 4 weeks after implantation of the pump and then were decapitated and blood was collected to measure plasma IGF-I level. The AVP-treated rats, 10 weeks after rAAV-AVP administration, and the untreated rats were also decapitated, and blood was collected.

Osmolality measurement and hormone assays. Plasma and urine osmolality was measured with an Advanced Osmometer 3W2 (Advanced Instruments, Needham Heights, MA). AVP levels of the culture supernatants, plasma, and neurohypophyseal extracts were measured with a commercially available RIA kit (Mitsubishi Chemical Co., Ibaraki, Japan) after extraction with a Sep-Pack C18 cartridge (Waters Corp., Milford, MA). Plasma levels of IGF-I were determined with a commercially available RIA kit (Diagnostic Systems Laboratories, Inc., Webster, TX).

Immunohistochemistry. The brains were cut to a thickness of 40 μm on a cryostat. The sections were incubated in rabbit IgG directed against AVP (1:5000 dilution; Chemicom International, Temecula, CA) for 48 h at 4°C and then subjected to endogenous peroxidase deactivation (15 min incubation with PBS containing 20% MeOH, 0.2% Triton X-100, and 1.5% H_2O_2). Bound primary antibody was detected by incubation for 24 h at 4°C with goat anti-rabbit IgG peroxidase complex (1:1000; Vector Laboratories, Inc., Burlingame, CA). Immunostaining was visualized using the DAB–glucose oxidase method.

Statistical analysis. All values were expressed as means ± SD. Statistical analysis was performed with the Student *t* test, ANOVA, or repeated-measure ANOVA followed by the Fisher least significant difference test.

Acknowledgments

We thank Avigen, Inc., for providing the AAV vector production system. We also thank Hartwig Schmale and Dietmar Richter (University of Hamburg) for providing wild-type AVP cDNA. This study was supported in part by grants from the Ministry of Health, Labor, and Welfare of Japan; by a Grant-in-Aid for Scientific Research on Priority Areas; and by Special Coordination Funds from the Ministry of Education, Culture, Sports, Science, and Technology of Japan and by a J.M.S. Graduate Student Research Award.

RECEIVED FOR PUBLICATION FEBRUARY 4, 2003; ACCEPTED AUGUST 14, 2003.

References

1. Davidson, B. L., Allen, E. D., Kozarsky, K. F., Wilson, J. M., and Roessler, B. J. (1993). A model system for in vivo gene transfer into the central nervous system using an adenoviral vector. *Nat. Genet.* **3**: 219–223.
2. Akli, K. S., *et al.* (1993). Transfer of a foreign gene into the brain using adenovirus vectors. *Nat. Genet.* **3**: 224–228.
3. Bajocchi, G., Feldman, S. H., Crystal, R. G., and Mastrangeli, A. (1993). Direct in vivo gene transfer to ependymal cells in the central nervous system using recombinant adenovirus vectors. *Nat. Genet.* **3**: 229–234.
4. Salle, G. L., *et al.* (1993). An adenovirus vector for gene transfer into neurons and glia in the brain. *Science* **259**: 988–990.
5. Kaplitt, M. G., *et al.* (1994). Long-term gene expression and phenotypic correction using adeno-associated virus vectors in the mammalian brain. *Nat. Genet.* **8**: 148–154.
6. Lo, W. D., *et al.* (1999). Adeno-associated virus-mediated gene transfer to the brain: duration and modulation of expression. *Hum. Gene Ther.* **10**: 201–213.
7. Naldini, L., *et al.* (1996). In vitro gene delivery and stable transduction of nondividing cells by a lentiviral vector. *Science* **272**: 263–267.
8. Fan, D., *et al.* (1998). Behavioral recovery in 6-hydroxydopamine-lesioned rats by cotransduction of striatum with tyrosine hydroxylase and aromatic l-amino acid decarboxylase genes using two separate adeno-associated virus vectors. *Hum. Gene Ther.* **9**: 2527–2535.
9. Shen, Y., *et al.* (2000). Triple transduction with adeno-associated virus vectors expressing tyrosine hydroxylase, aromatic-l-amino-acid decarboxylase, and GTP cyclohydrolase for gene therapy of Parkinson's disease. *Hum. Gene Ther.* **11**: 1509–1519.
10. Kordower, J. H., *et al.* (2000). Neurodegeneration prevented by lentiviral vector delivery of GDNF in primate models of Parkinson's disease. *Science* **290**: 767–773.
11. Muramatsu, S., *et al.* (2002). Behavioral recovery in a primate model of Parkinson's disease by triple transduction of striatal cells with adeno-associated viral vectors expressing dopamine-synthesizing enzymes. *Hum. Gene Ther.* **13**: 345–354.
12. Geddes, B. J., Harding, T. C., Lightman, S. L., and Uney, J. B. (1999). Assessing viral gene therapy in neuroendocrine models. *Front. Neuroendocrinol.* **20**: 296–316.
13. Valtin, H. (1982). The discovery of the Brattleboro rat, recommended nomenclature, and the question of proper controls. *Ann. N. Y. Acad. Sci.* **394**: 1–9.
14. Robertson, G. L., and Athar, S. (1976). The interaction of blood osmolality and blood volume in regulating plasma vasopressin in man. *J. Clin. Endocrinol. Metab.* **42**: 613–620.
15. Robertson, G. L., Aycinema, P., and Zebra, R. L. (1982). Neurogenic disorders of osmoregulation. *Am. J. Med.* **72**: 339–353.
16. Dunn, F. L., Brennan, T. J., Nelson, A. E., and Robertson, G. L. (1973). The role of blood osmolality and volume in regulating vasopressin secretion in the rat. *J. Clin. Invest.* **52**: 3212–3219.
17. Stricker, E. M., and Verbalis, J. G. (1986). Interaction of osmotic and volume stimuli in regulation of neurohypophyseal secretion in rats. *Am. J. Physiol.* **250**: R267–R275.
18. Schmale, H., Heinsohn, S., and Richter, D. (1983). Structural organization of the rat gene for the arginine vasopressin–neurophysin precursor. *EMBO J.* **2**: 763–767.
19. Brownstein, M. J., Russell, J. T., and Gainer, R. H. (1980). Synthesis, transport, and release of posterior pituitary hormones. *Science* **207**: 373–378.
20. Schmale, H., and Richter, D. (1984). Single base deletion in the vasopressin gene is the cause of diabetes insipidus in Brattleboro rats. *Nature* **308**: 705–709.
21. Jirikowski, G. F., Sanna, P. P., Machiesewski-Lenoir, D., and Bloom, F. E. (1992). Reversal of diabetes insipidus in Brattleboro rats: intrahypothalamic injection of vasopressin mRNA. *Science* **255**: 996–998.
22. Maciejewski-Lenoir, D., Jirikowski, G. F., Sanna, P. P., and Bloom, F. E. (1993). Reduction of exogenous vasopressin RNA poly(A) tail length increase its effectiveness in

doi:10.1016/j.ymthe.2003.08.019

transiently correcting diabetes insipidus in the Brattleboro rat. *Proc. Natl. Acad. Sci. USA* **90**: 1435–1439.
23. Geddes, B. J., Harding, T. C., Lightman, S. L., and Uney, J. B. (1997). Long-term gene therapy in the CNS: reversal of hypothalamic diabetes insipidus in the Brattleboro rat by using an adenovirus expressing arginine vasopressin. *Nat. Med.* **3**: 1402–1404.
24. Bienemann, A. S., *et al.* (2003). Long-term replacement of a mutated nonfunctional CNS gene: reversal of hypothalamic diabetes insipidus using an EIAV-based lentiviral vector expressing arginine vasopressin. *Mol. Ther.* **7**: 588–596.
25. Blacklow, N. R., Hoggan, M. D., Kapikian, A. Z., Austin, J. B., and Rowe, W. P. (1968). Epidemiology of adenovirus-associated virus infection in a nursery population. *Am. J. Epidemiol.* **88**: 368–378.
26. Sokol, H. W., and Sise, J. (1973). The effect of exogenous vasopressin and growth hormone on the growth of rats with hereditary hypothalamic diabetes insipidus. *Growth* **37**: 113–117.
27. Bullier-Picard, F., *et al.* (1986). The Brattleboro rat: normal growth hormone secretion, decreased hepatic growth hormone receptors and low plasma somatomedin activity. *Mol. Cell. Endocrinol.* **45**: 49–56.
28. Sonnemans, M. A. F., Evans, D. A. P., Burbach, J. P. H., and van Leeuwen, F. W. (1996). Immunocytochemical evidence for the presence of vasopressin in intermediate sized neurosecretory granules of solitary neurohypophyseal terminals in the homozygous Brattleboro rat. *Neuroscience* **72**: 225–231.
29. Seidah, N. G., and Chretien, M. (1999). Proprotein and prohormone convertases: a family of subtilases generating diverse bioactive polypeptides. *Brain Res.* **848**: 45–62.
30. Davidson, S. L., *et al.* (2000). Recombinant adeno-associated virus type 2, 4 and 5 vectors: transduction of variant cell types and regions in the mammalian central nervous system. *Proc. Natl. Acad. Sci. USA* **97**: 3428–3432.
31. Landgraph, R., Neumann, I., and Schwartzberg, H. (1988). Central and peripheral release of vasopressin and oxytocin in the conscious rat after osmotic stimulation. *Brain Res.* **457**: 219–225.
32. Burbach, J. P. H., *et al.* (1984). Differential response to osmotic stress of vasopressin–neurophysin mRNA in hypothalamic nuclei. *Neuroendocrinology* **39**: 582–584.
33. Linton, E. A., *et al.* (1985). Stress-induced secretion of adrenocorticotropin in rats is inhibited by administration of antisera to ovine corticotropin releasing factor and vasopressin. *Endocrinology* **116**: 966–970.
34. Sherman, T. G., Civelli, O., Douglass, J., Herbert, E., and Watson, S. J. (1986). Coordinate expression of hypothalamic pro-dynorphin and pro-vasopressin mRNA with osmotic stimulation. *Neuroendocrinology* **44**: 222–228.
35. Bisset, G. W., and Chowdrey, H. S. (1988). Control of release of vasopressin by neuroendocrine reflexes. *Q. J. Exp. Physiol.* **73**: 811–872.
36. Bartanusz, V., *et al.* (1993). Stress-induced increase in vasopressin and corticotropin-releasing factor expression in hypophysiotropic paraventricular neurons. *Endocrinology* **132**: 895–902.
37. Lederis, K., and Jayasena, K. (1970). Storage of neurohypophyseal hormones and the mechanism for their release). *Pharmacology of the Endocrine System and Related Drugs: The Neurohypophysis* (In *H. Heller, and B. T. Pickering, Eds.), pp. 111–154. Pergamon, London/Oxford.*
38. Gainer, H., Sarne, Y., and Brownstein, M. J. (1977). Biosynthesis and axonal transport of rat neurohypophyseal proteins and peptides. *J. Cell Biol.* **73**: 366–381.
39. Robinson, A. G., and Fitzsimmons, M. D. (1995). Stimulation–translation coupling in the vasopressin system). *Neurohypophysis* (In *T. Saito, K. Kurokawa, and S. Yoshida, Eds.), pp. 187–194. Elsevier, Amsterdam.*
40. Shoji, M., *et al.* (1994). Effects of acute salt loading on vasopressin mRNA level in the rat brain. *Am. J. Physiol.* **266**: R1591–R1595.
41. Arima, H., *et al.* (1999). Rapid and sensitive vasopressin heteronuclear RNA response to changes in plasma osmolality. *J. Neuroendocrinol.* **11**: 337–341.
42. Poulain, D. A., and Wakerley, J. B. (1982). Electrophysiology of hypothalamic magnocellular neurons secreting oxytocin and vasopressin. *Neuroscience* **7**: 773–808.
43. Dyball, R. E. J. (1982). Spike activity in "vasopressin" neurons in the Brattleboro rat. *Ann. N. Y. Acad. Sci.* **394**: 128–134.
44. Matsushita, T., *et al.* (1998). Adeno-associated virus vectors can be efficiently produced without helper virus. *Gene Ther.* **5**: 938–945.
45. Paxinos, G., and Watson, C. (1986). The Rat Brain in Stereotaxic Coordinates,. 2nd ed. Academic Press, San Diego, CA.

THE JOURNAL OF GENE MEDICINE
J Gene Med 2003; 5: 921–928.
Published online 20 June 2003 in Wiley InterScience (www.interscience.wiley.com). DOI: 10.1002/jgm.431

RESEARCH ARTICLE

Efficient gene transfer of a simian immunodeficiency viral vector into cardiomyocytes derived from primate embryonic stem cells

Mihoko Nagata,[1] Masafumi Takahashi,[2,4]* Shin-ichi Muramatsu,[1]* Yasuji Ueda,[7] Yutaka Hanazono,[5] Koichi Takeuchi,[6] Koji Okada,[3] Yutaka Suzuki,[8] Yasushi Kondo,[8] Masafumi Suemori,[9] Uichi Ikeda,[2] Imaharu Nakano,[1] Eiji Kobayashi,[4] Mamoru Hasegawa,[7] Keiya Ozawa,[5] Norio Nakatsuji[9,10] and Kazuyuki Shimada[2]

[1]*Division of Neurology, Department of Medicine, Jichi Medical School, Tochigi 329-0498, Japan;* [2]*Division of Cardiology, Department of Medicine, Jichi Medical School, Tochigi 329-0498, Japan;* [3]*Division of Endocrinology, Department of Medicine, Jichi Medical School, Tochigi 329-0498, Japan;* [4]*Division of Organ Replacement Research, Center for Molecular Medicine, Jichi Medical School, Tochigi 329-0498, Japan;* [5]*Division of Genetic Therapeutics, Center for Molecular Medicine, Jichi Medical School, Tochigi 329-0498, Japan;* [6]*Department of Anatomy, Jichi Medical School, Tochigi 329-0498, Japan;* [7]*DNAVEC Research, Inc., Ibaraki 305-0856, Japan;* [8]*Tanabe Seiyaku Co., Ltd., Osaka 532-8505, Japan;* [9]*Department of Development and Differentiation, Institute for Frontier Medical Sciences, Kyoto University, Kyoto 606-8507, Japan;* [10]*Stem Cell Research Center, Institute for Frontier Medical Sciences, Kyoto University, Kyoto 606-8507, Japan*

*Correspondence to: Masafumi Takahashi or Shin-ichi Muramatsu, Division of Organ Replacement Research or Division of Neurology, Jichi Medical School, Minamikawachi-machi, Tochigi 329-0498, Japan. E-mail: masafumi@jichi.ac.jp or muramats@jichi.ac.jp

Received: 18 December 2002
Revised: 7 April 2003
Accepted: 5 May 2003

Abstract

Background Embryonic stem (ES) cells continually proliferate and can generate large numbers of differentiated cells. Genetic manipulation of transplantable cells derived from primate ES cells offers considerable potential for development research and regenerative cell therapy. However, protocols for efficient gene transfer into primate ES-cell-derived cells have not yet been established.

Methods Spontaneously contracting areas were derived from cynomolgus monkey ES cells. Features of cardiomyocytes in the area were analyzed according to gene expression (RT-PCR), morphology (immunostaining and electron microscopy), and function (intracellular calcium transience). Beating cells were transduced using a simian immunodeficiency virus (SIV) vector expressing enhanced green fluorescence protein (EGFP), then transplanted into ischemic rat myocardium.

Results Beating cells derived from monkey ES cells displayed gene expression, ultrastructural and functional properties of early-stage cardiomyocytes. Highly efficient (97% cardiac phenotype) and stable transduction of these ES-cell-derived cardiomyocytes was achieved using SIV vector without altering contractile function. In addition, transduced cardiomyocytes survived in the myocardium of a rat myocardial infarction model.

Conclusions A lentiviral vector system based on SIV represents a useful vehicle for genetic modification of cardiomyocytes derived from primate ES cells, and can extend the application of primate ES cells to gene therapy.

Keywords embryonic stem cell; cardiomyocyte; simian immunodeficiency virus; cell transplantation; myocardial infarction

Introduction

The generation of various differentiated cells from pluripotent embryonic stem (ES) cells provides a renewable resource not only for studying the mechanism of early development *in vitro*, but also for cell transplantation therapy. Among many specialized cells in adults, cardiomyocytes are terminally differentiated and have no or only limited regenerative capacity after injury such as myocardial infarction [1]. Thus, the transplantation of functional cardiomyocytes into the damaged myocardium would have therapeutic potential. Recent studies have demonstrated that human ES cells can differentiate into cardiomyocytes with structural and functional properties *in vitro* [2–5]. Although human ES cells hold promise for clinical applications, an alternative model system based on ES cells derived from

experimental animals may be necessary for pre-clinical studies, including allogenic transplantation. We established cynomolgus monkey (*Macaca fascicularis*) ES cell lines [6] that are similar to human ES cells but distinct from murine ES cells in terms of morphology, expression of surface markers, feeder- and leukemia inhibitory factor-dependence and other factors. These features indicate that cynomolgus ES cells represent a suitable pre-clinical model for cell transplantation therapy.

Gene transfer into transplantable cells has potential to enhance the effects of cell replacement therapy. Although murine ES cells can be transduced by electroporation or mouse stem cell virus (MSCV)-based retroviral vectors [7–9], primate ES cells are not efficiently transduced by these methods [10]. Lentiviral vectors can transduce both dividing and non-dividing cells and long-term expression of the transgene is stable in a wide range of target cells [11–13]. We have described the highly efficient transfer of a gene into cynomolgus monkey undifferentiated ES cells using a lentivirus vector based on simian immunodeficiency virus (SIV) [14].

The present study examines the differentiation of cynomolgus ES cells into functional cardiomyocytes and determines the efficiency and stability of gene transduction into these cardiomyocytes using an SIV-based lentiviral vector encoding the enhanced green fluorescence protein (EGFP) gene. We also evaluate the survival of transplanted cardiomyocytes derived from cynomolgus ES cells in the injured myocardium of a rat myocardial infarction model.

Materials and methods

Cell preparations

The cynomolgus monkey ES cell line CMK6 [6] was cultured in DMEM/F12 (Sigma, St. Louis, USA) on a mouse embryonic fibroblast feeder layer that was mitotically inactivated with mitomycin C (Kyowa, Tokyo, Japan). The medium was supplemented with 0.1 mM 2-mercaptoethanol (Sigma), 2 mM glutamine (Invitrogen, Carlsbad, USA), 1 mM sodium pyruvate (Invitrogen) and 15% fetal bovine serum (FBS, ICN Biomedicals, Inc., Ohio, USA). To induce differentiation, ES cells were dispersed into small clumps using collagenase IV (Wako, Osaka, Japan), transferred to plastic Petri dishes and suspension-cultured for 10 days. During this period, the cells aggregated to form embryoid bodies (EBs), which were then plated on plastic plates, and the appearance of spontaneous contractions was observed under a microscope. Rat neonatal cardiomyocytes were prepared from cardiac ventricles of 1-day-old Sprague-Dawley rats as described previously [15]. The cells were grown in DMEM (Sigma) supplemented with 10% FBS (ICN Biomedicals, Inc.), and 1% penicillin/streptomycin solution (Invitrogen). All experiments were carried out in full compliance with the institutional animal care and use committee of the Jichi Medical School.

RT-PCR

Total RNA from undifferentiated ES cells, contracting EBs, and heart tissue of an adult cynomolgus monkey that was killed for unrelated reasons was extracted using a RNA extraction kit (Qiagen, Hilden, Germany) according to the manufacturer's instructions. Complementary DNA synthesized from 1 μg total RNA using SuperScript II reverse transcriptase (Life Technologies, Gaithersburg, MD, USA) was amplified by PCR using the following primers selective for human cardiac genes (oligonucleotide sequences are given in brackets in the order of anti-sense, sense primer followed by the annealing temperature, cycles used for PCR and length of the amplified fragment): cardiac troponin T (cTnT, 5′-GGCAGCGGAAGAGGATGCTGAA and 5′-GAGGCACCAAGTTGGGCATGAACGA; 60 °C; 35 cycles; 150 bp), atrial myosin light chain (MLC-2A, 5′-ACAGAGTTTATTGAGGTGCCCC and 5′-AAGGTGAAGTG-TCCCAGAGG; 61 °C; 35 cycles; 381 bp), ventricular myosin light chain (MLC-2V, 5′-TATTGGAACATGGCCTC-TGGAT and 5′-GGTGCTGAAGGCTGATTACGTT; 61 °C; 35 cycles; 382 bp), α-myosin heavy chain (αMHC, 5′-GTCATTGCTGAAACCGAGAATG and 5′-GCAAAGTACTG-GATGACACGCT; 61 °C; 40 cycles; 413 bp), octamer-binding protein 4 (Oct-4, 5′-GAGAACAATGAGAACCTTC-AGGAGA and 5′-TTCTGGCGCCGGTTACAGAACCA; 55 °C; 35 cycles; 219 bp), and glyceraldehyde-3-phosphate dehydrogenase (GAPDH, 5′-ATGCCAGTGAGCTTCCCGTT and 5′-CATCACCATCTTCCAGGAGC; 58 °C; 30 cycles; 473 bp).

Electron microscopy

For transmission electron microscopy, tissues were fixed in 2% paraformaldehyde/2.5% glutaraldehyde in 0.1 M phosphate-buffered saline (PBS), pH 7.4, at 4 °C for 24 h, postfixed in 1% OsO_4 in PBS for 1 h, dehydrated in a graded ethanol series and embedded in Epon 812. Thin (60–90 nm) sections were stained with uranyl acetate and lead citrate, and observed using a JEM-2000EX transmission electron microscope operating at 80 kV.

Intracellular calcium transience

Intracellular calcium transience of the EBs and rat neonatal cardiomyocytes was measured as described previously [16]. Briefly, cells were loaded with fura-2-AM (Dojin Biochemicals, Kumamoto, Japan), washed and transferred to the chamber of a fluorescence spectrophotometer (CAF-100; Japan Spectroscopic Co., Tokyo, Japan). Fura-2 fluorescence was measured using a dual wavelength system. Fluorescence was monitored at 500 nm, with excitation at 340 and 380 nm in the ratio mode. After achieving a stable fluorescence signal, the cells were stimulated with 100 nM angiotensin II (Sigma) or endothelin-1 (Peptide Institute Inc., Osaka, Japan). The cells pretreated with [Sar^1,Ile^8]-angiotensin II (non-selective antagonist; Peptide Institute Inc.) or CV-11 974

(angiotensin II type 1 receptor antagonist; kind gift from Takeda Chemical Industries, Ltd., Osaka, Japan) were also stimulated with angiotensin II.

Immunohistochemical staining

Contracting areas in EBs were mechanically dissected using a sterile micropipette. The samples were fixed in 4% paraformaldehyde in 0.1 M PBS (pH 7.4) containing 8% sucrose at 4 °C for 4 h, washed with PBS containing 10, 20, and 30% sucrose in that order, embedded in OCT compound (Miles Laboratory, IN, USA), frozen in liquid nitrogen and cut into thin (8–10 μm) sections. We incubated the sections with monoclonal antibodies against human cardiac troponin I (cTnI) and cardiac myosin (both from Biogenesis, England, UK; diluted 1 : 200) for 1 h at room temperature. These anti-human antibodies cross-react against cynomolgus monkey cardiomyocytes but not against rat cardiomyocytes. Texas red labelled anti mouse IgG (Vector, Burlingame, CA, USA) was the secondary antibody. Samples were fixed in 4% paraformaldehyde in PBS for 20 min and immersed in 4′,6-diamidino-2-phenylindole (DAPI, 500 ng/ml; Sigma) containing Tris buffer (pH 7.4) for 10 min at room temperature to stain nuclei.

Vector construction and transduction

The SIV vector expressing the EGFP gene (Clontech, CA, USA) was produced by transient transfection into 293T cells as described [17]. Briefly, the envelope plasmid (pVSV-G; Clontech) encoding the vesicular stomatitis virus G (VSV-G) protein, the packaging plasmid (pCAGGS/Sagm-gtr), and the vector plasmid (pBS/CG2-Rc/s-CMV-ΔU) expressing the EGFP gene under the control of the cytomegalovirus (CMV) promoter were transfected into 293T cells and supernatants were harvested 48 h later. The SIV vector was concentrated by centrifugation of the supernatants at 42 500 *g* for 90 min and the titer assessed by fluorescence activated cell sorting (FACS) using 293T cells as targets was 1.87×10^8 TU/ml.

Spontaneously contracting EBs were transduced with SIV vector expressing the EGFP gene at a multiplicity of infection (MOI) of 100. Cells were washed with PBS 10 h later and incubated in fresh medium for 7–14 days. Contracting EBs were micro-dissected with a sterile micropipette and prepared for immunohistological analysis. Other dissected cells were enzymatically dispersed in trypsin/EDTA solution (0.05% trypsin, 0.53 mM EDTA; Invitrogen) for 7 min at 37 °C and resuspended in DMEM/F12 for use in cell transplantation experiments. To determine the transduction efficiency with the SIV vector, some dissociated cells were centrifuged with Cytospin and stained with anti-cTnI antibody. We then calculated the ratio (%) of EGFP-positive cells among cTnI-immunoreactive cells.

Cell transplantation in a rat myocardial infarction model

Immunodeficient (F344/N *rnu/rnu*) nude rats (male, initial body weight 140–180 g) were used (n = 4) to avoid graft-versus-host disease. Left thoracotomy proceeded under general anesthesia, then the pericardium was opened and the left descending coronary artery was ligated. Cynomolgus ES-cell-derived cardiomyocytes expressing EGFP (1×10^5 cells/50 μl) were implanted in the injured myocardium 30 min after myocardial infarction induction. Two weeks later, rats were killed and hearts were extracted for immunohistological study. All experiments in this study were performed in accordance with the Jichi Medical School Guide for Laboratory Animals.

Statistical analysis

Results are presented as mean ± SD. For comparisons between multiple groups, we determined the significance of differences between group means by ANOVA using the least significant difference for multiple comparisons. Differences at values of $p < 0.05$ were considered to be statistically significant.

Results

Differentiation of cynomolgus ES cells into cardiomyocytes

Rhythmically contracting areas appeared between 3 and 10 days after plating EBs on plastic plates, and were maintained for 3–4 weeks. Figure 1A shows that the ratio of EBs containing beating areas as a function of time after plating was 8.7% (of 751 EBs) at 14 days.

We investigated the expression of cardiac-specific genes in spontaneously contracting EBs. The RT-PCR results revealed that these cells expressed cTnT, MLC-2A, MLC-2V, and αMHC (Figure 1B). In contrast, Oct-4, a marker of undifferentiated ES cells, was expressed in undifferentiated ES cells, but not in contracting EBs or cynomolgus heart tissues. Light microscopy showed that the contracting areas were composed mainly of round or rod-shaped mononuclear cells. Myofibers were detected in the high power light microscopy image stained with toluidine blue (Figure 2A). Transmission electron microscopy revealed that these cells had the mature sarcomeric organization and desmosome structure of cardiomyocytes (Figures 2B–2D). To further elucidate whether these cells have functional features as cardiomyocytes, we measured the effect of angiotensin II or endothelin-1 on intracellular calcium transience. Intracellular calcium transience was obviously stimulated with angiotensin II or endothelin-1. The angiotensin II stimulated effect was completely inhibited by pretreatment with [Sar^1,Ile^8]-angiotensin II

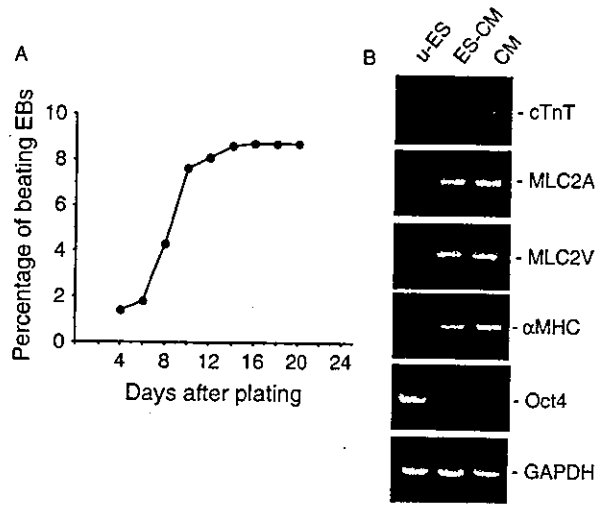

Figure 1. Differentiation of cardiomyocytes from cynomolgus ES cells. (A) Cumulative ratio of EBs derived from cynomolgus ES cells containing spontaneously contracting areas during differentiation. (B) Expression of specific cardiac markers. RNA samples from undifferentiated ES cells (u-ES), contracting area of EBs (ES-CM), and cynomolgus monkey cardiac tissues (CM) analyzed by RT-PCR for the expression of cardiac-specific markers: cTnT, MLC-2A, MLC-2V and αMHC. Oct-4 is undifferentiated ES cell marker. GAPDH served as internal standard

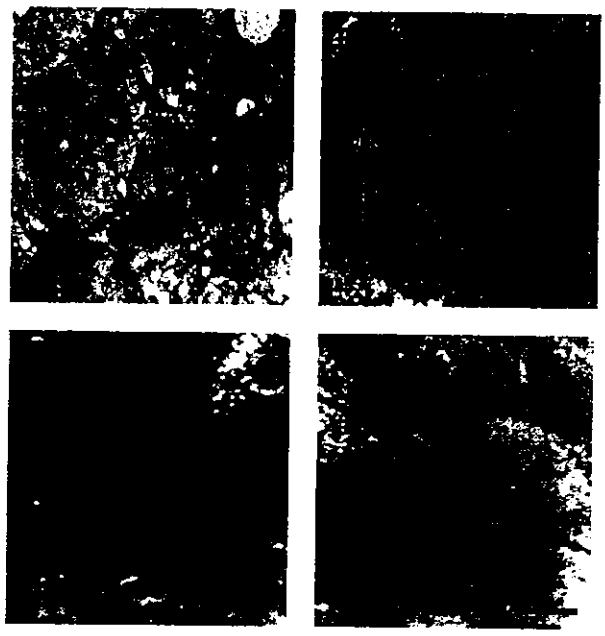

Figure 2. Morphological analysis of contracting EBs 14 days after plating. (A) High power light microscopy image stained with toluidine blue. Myofibers were observed (arrows). Magnification ×1000. (B) Low power transmission micrograph revealed sarcomeric organization (arrowheads) and desmosomes (arrows). Scale bar: 2 μm. (C, D) High power transmission micrograph. Sarcomeric organization (C) and desmosomes (D, arrows) are evident. Scale bar: 500 nm

or CV-11 974 (Figure 3). We also confirmed the expression of cTnI and cardiac myosin in the contracting EBs by immunohistochemical staining (Figures 4B and 4E). Taken together, these results indicate that cynomolgus ES cells differentiate into cardiomyocytes *in vitro*.

Transgene expression with a SIV-based lentiviral vector

We used SIV vectors encoding the EGFP gene under the control of the CMV promoter to examine gene transduction in cardiomyocytes derived from ES cells. We detected EGFP expression in cultures by 5 days and this was maintained for at least 28 days (data not shown). Most staining of the transduced cells overlapped with cTnI or cardiac myosin (Figures 4C and 4F). The ratio (%) of EGFP-positive cells among cTnI-positive cells (4276 cells in eight samples) reached 97.1 ± 1.8% at 14 days after transduction (Figure 5). Cardiac differentiation and contractile function were not significantly altered in infected cultures.

Transplantation of cardiomyocytes derived from cynomolgus ES cells

We further investigated whether cardiomyocytes derived from cynomolgus monkey ES cells can survive in the rat myocardial infarction model myocardium. Transplanted cells transduced with the EGFP-SIV vector were identified in myocardial tissue section by green fluorescence, while cells stained with the cardiac-specific marker cTnI were identified by red fluorescence. The myocardial tissue co-expressed cTnI and EGFP 14 days after cell transplantation (Figure 6). In addition, the cTnI- and EGFP-expressed cells were normally stained with DAPI. These results confirmed that cardiomyocytes derived from transplanted ES cells survived in the injured myocardium.

Discussion

The present study demonstrates that cynomolgus monkey ES cells can differentiate into cardiomyocytes *in vitro*. Cardiomyocytic nature was confirmed by (1) the expression of cardiomyocyte-specific molecular markers such as cTnT, MLC-2A, MLC-2V, and αMHC, (2) the ultrastructural features of sarcomeric organization and desmosomes, and (3) intracellular calcium transience. Our cynomolgus ES cells formed contracting areas 3 days after EBs were plated. This point is in between the 1 day for murine ES cells and the 5–8 days for human ES cells after plating [2], reflecting the fetal developmental periods of these three species.

Transplantation of viable cardiomyocytes has emerged as a potential new therapy with which to treat the injured myocardium. Various types of cells including fetal and neonatal cardiomyocytes [18–20], skeletal myoblasts [21–23], and bone marrow cells [24,25] have been used as donor cells. However, the source of these cells might be limited and insufficient for clinical purposes. In

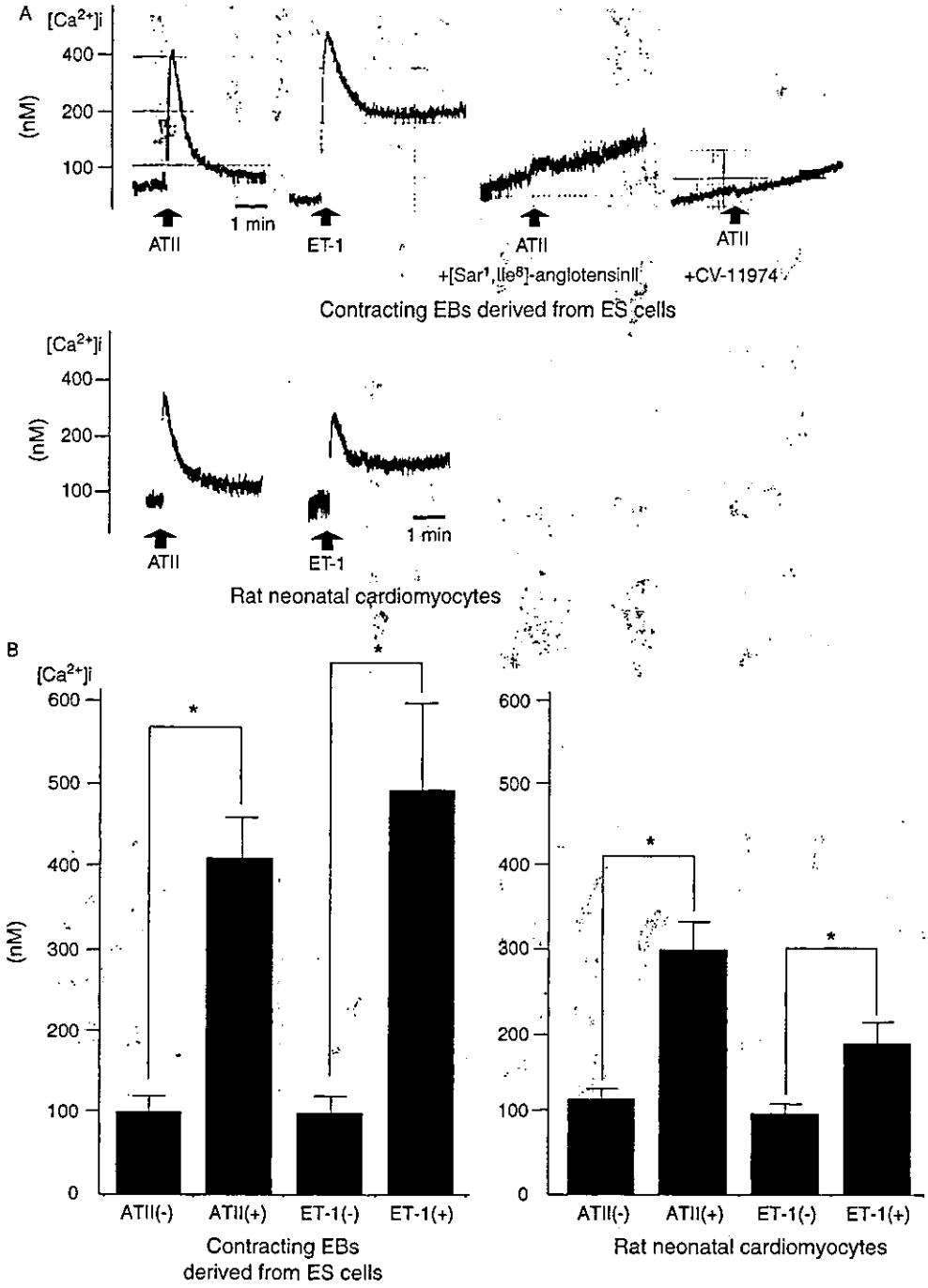

Figure 3. Functional analysis. Intracellular Ca^{2+} transience ($[Ca^{2+}]i$) of contracting EBs and rat neonatal cardiomyocytes determined by fura-2 fluorescence. (A) Typical Ca^{2+} transience appeared in response to 100 nM angiotensin II (ATII) and endothelin-1 (ET-1) in both cell types. The angiotensin-II-stimulated Ca^{2+} transience was inhibited by treatment with [Sar^1,Ile^8]-angiotensin II (non-selective antagonist) or CV-11974 (angiotensin II type 1 receptor selective antagonist) in contracting EBs. (B) Bar graph shows mean ± SD (n = 40). *$p < 0.05$

addition, significant proportions of transplanted cells die after transplantation [26]. Since ES cells have a potent proliferative capacity, cardiomyocytes derived from ES cells are good candidates for cell transplantation therapy [4,27–29]. Cardiomyocytes derived from murine ES cells survive after intracardiac implantation [30]. We have shown here that cardiomyocytes derived from primate ES cells can also survive in the myocardium of myocardial infarction rats.

To enhance the effects of cell transplantation therapy, gene modification of the donor cells might be useful for treating cardiac diseases. Angiogenic agents such as vascular endothelial growth factor (VEGF) and basic fibroblast growth factor (bFGF) might be candidates for gene transfer as they attenuate myocardial ischemia in patients with ischemic heart disease when administrated either into myocardium as a naked plasmid [31] or into coronary artery as a recombinant protein [32]. We used

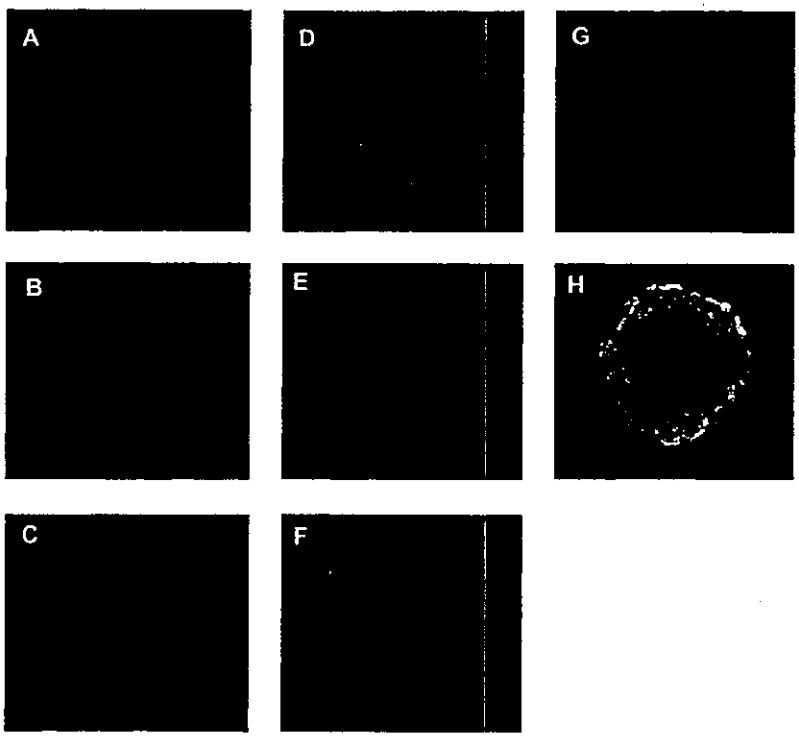

Figure 4. Immunohistochemical staining and EGFP expression. Cardiomyocytes derived from cynomolgus ES cells were transduced with EGFP-SIV vector. Contracting areas were isolated and stained with DAPI (A, D), cTnI (B) and cardiac myosin (E), then EGFP expression (C, F) was identified by fluorescent microscopy. Control staining in which mouse non-specific IgG was used as a primary antibody (G) and phase-contrast photograph (H). Magnification ×100

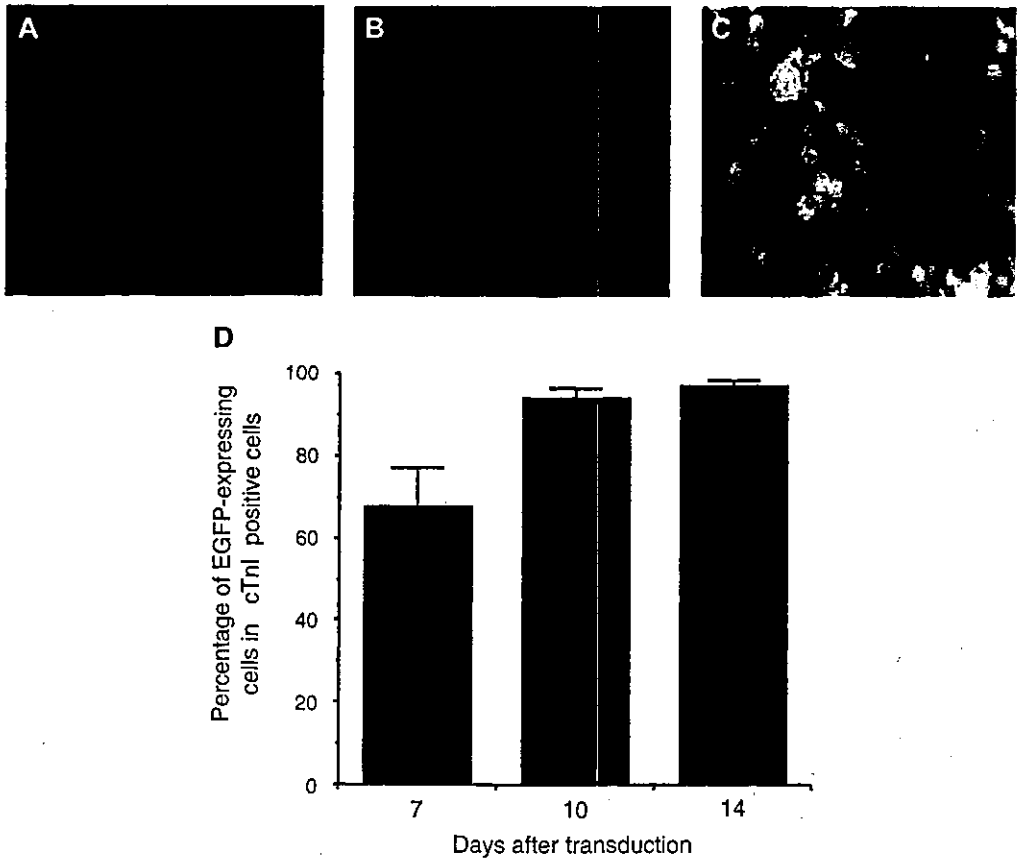

Figure 5. Transgene expression using SIV-based lentivirus vector. Cardiomyocytes derived from cynomolgus ES cells were transduced with EGFP-SIV vector. Contracting areas were isolated, trypsinized and stained with cTnI (A), then EGFP expression (B) was identified by fluorescent microscopy. (C) B merged with A. Magnification ×200. (D) Ratio (%) of cells expressing EGFP in cTnI-positive cells. Values are means ± SD of eight independent experiments

Figure 6. Expression of cTnI and EGFP in myocardium transplanted with cardiomyocytes derived from ES cells. Cardiomyocytes derived from cynomolgus ES cells transduced with the EGFP-SIV vector were implanted into injured myocardium. (A) DAPI staining, (B) cTnI staining, and (C) EGFP expression. Bar: 50 μm

a lentiviral vector based on SIV derived from the African green monkey (SIVagm) [17]. Lentiviral vectors based on either human immunodeficiency virus type 1 (HIV-1) or SIVagm are the only gene delivery vehicles that can efficiently transduce primate ES cells [14,33]. SIVagm-based vectors could offer safety advantages over those based on HIV-1 in human gene therapy. SIVagm is non-pathogenic in its natural host and in experimentally inoculated macaque monkeys, whereas HIV-1 causes severe pathogenicity in humans. In addition to the low homology of sequences between HIV-1 and SIVagm, most viral sequences were removed from our SIVagm vectors. Thus, this vector is unlikely to generate replication-competent virus by recombination between the two types of viruses in humans.

We efficiently and stably expressed EGFP in cardiomyocytes derived from cynomolgus ES cells using a lentiviral vector system based on SIV. Furthermore, we demonstrated that the implanted EGFP-positive cardiomyocytes derived from ES cells survived in the injured rat myocardium. Cell transplantation together with lentivirus-mediated gene modification offers considerable potential as a new therapeutic approach to treating cardiac diseases.

Acknowledgements

We thank Naomi Takino, Chieko Muramatsu, and Yuki Onuma for excellent technical assistance. This study was supported by Special Coordination Funds for Promoting Science and Technology from the Ministry of Education, Science, Sports and Culture, the Japanese Government; by a Grant-in-Aid for the Development of Innovative Technology, the Kanae Foundation for Life and Socio-Medical Science; and by funds from The Cell Science Research Foundation.

References

1. Anversa P, Fitzpatrick D, Argani S, *et al.* Myocyte mitotic division in the aging mammalian rat heart. *Circ Res* 1991; 69: 1159–1164.
2. Kehat I, Kenyagin-Karsenti D, Snir M, *et al.* Human embryonic stem cells can differentiate into myocytes with structural and functional properties of cardiomyocytes. *J Clin Invest* 2001; 108: 407–414.
3. Xu C, Police S, Rao N, *et al.* Characterization and enrichment of cardiomyocytes derived from human embryonic stem cells. *Circ Res* 2002; 91: 501–508.
4. Boheler KR, Czyz J, Tweedie D, *et al.* Differentiation of pluripotent embryonic stem cells into cardiomyocytes. *Circ Res* 2002; 91: 189–201.
5. Kehat I, Gepstein A, Spira A, *et al.* High-resolution electrophysiological assessment of human embryonic stem cell-derived cardiomyocytes: a novel in vitro model for the study of conduction. *Circ Res* 2002; 91: 659–661.
6. Suemori H, Tada T, Torii R, *et al.* Establishment of embryonic stem cell lines from cynomolgus monkey blastocysts produced by IVF or ICSI. *Dev Dyn* 2001; 222: 273–279.
7. Cherry SR, Biniszkiewicz D, van Parijs L, *et al.* Retroviral expression in embryonic stem cells and hematopoietic stem cells. *Mol Cell Biol* 2000; 20: 7419–7426.
8. Grez M, Akgun E, Hilberg F, *et al.* Embryonic stem cell virus, a recombinant murine retrovirus with expression in embryonic stem cells. *Proc Natl Acad Sci U S A* 1990; 87: 9202–9206.
9. Loh TP, Sievert LL, Scott RW. Evidence for a stem cell-specific repressor of Moloney murine leukemia virus expression in embryonal carcinoma cells. *Mol Cell Biol* 1990; 10: 4045–4057.
10. Eiges R, Schuldiner M, Drukker M, *et al.* Establishment of human embryonic stem cell-transfected clones carrying a marker for undifferentiated cells. *Curr Biol* 2001; 11: 514–518.
11. Blomer U, Naldini L, Kafri T, *et al.* Highly efficient and sustained gene transfer in adult neurons with a lentivirus vector. *J Virol* 1997; 71: 6641–6649.
12. Kafri T, Blomer U, Peterson DA, *et al.* Sustained expression of genes delivered directly into liver and muscle by lentiviral vectors. *Nat Genet* 1997; 17: 314–317.
13. Miyoshi H, Takahashi M, Gage FH, *et al.* Stable and efficient gene transfer into the retina using an HIV-based lentiviral vector. *Proc Natl Acad Sci U S A* 1997; 94: 10319–10323.
14. Asano T, Hanazono Y, Ueda Y, *et al.* Highly efficient gene transfer into primate embryonic stem cells with a simian lentivirus vector. *Mol Ther* 2002; 6: 162–168.
15. Kamitani T, Ikeda U, Muto S, *et al.* Regulation of Na, K-ATPase gene expression by thyroid hormone in rat cardiocytes. *Circ Res* 1992; 71: 1457–1464.
16. Okada K, Ishikawa S, Saito T. Enhancement of intracellular sodium by vasopressin in spontaneously hypertensive rats. *Hypertension* 1993; 22: 300–305.
17. Nakajima T, Nakamaru K, Ido E, *et al.* Development of novel simian immunodeficiency virus vectors carrying a dual gene expression system. *Hum Gene Ther* 2000; 11: 1863–1874.
18. Scorsin M, Marotte F, Sabri A, *et al.* Can grafted cardiomyocytes colonize peri-infarct myocardial areas? *Circulation* 1996; 94: II337–340.
19. Li RK, Jia ZQ, Weisel RD, *et al.* Cardiomyocyte transplantation improves heart function. *Ann Thorac Surg* 1996; 62: 654–660; discussion 660–661.
20. Reinecke H, Zhang M, Bartosek T, *et al.* Survival, integration, and differentiation of cardiomyocyte grafts: a study in normal and injured rat hearts. *Circulation* 1999; 100: 193–202.
21. Yoon PD, Kao RL, Magovern GJ. Myocardial regeneration. Transplanting satellite cells into damaged myocardium. *Tex Heart Inst J* 1995; 22: 119–125.